A first step to the rational design of an organometallic catalyst: $Rh_xH_ySn_z(CH_3)_n$

A.H. Jubert [a], M.C. Michelini [a], G.L. Estiú [a] and O.A. Ferretti [b]

[a] *CEQUINOR, Facultad de Ciencias Exactas, UNLP, CC 962, 1900 La Plata, Argentina*
[b] *CINDECA and Departamento de Ingeniería Química, Facultad de Ingeniería, UNLP, 47 Nro 257, CC 59, 1900 La Plata, Argentina*

Received 28 August 1996; accepted 1 May 1997

Geometry optimization procedures and electronic structure SCF/MRCI calculations of the intermediate neglect differential overlap (INDO) type are used to study the interaction between a $Sn(CH_3)_4$ molecule and a reduced hydrogenated Rh_{13} I_h cluster, whose importance is associated to the formation of an active and selective catalytic phase for hydrogenation processes. According to the calculations, the reaction mechanism implies the initial adsorption of alkyl tin to a Rh atom of the hydrogenated metal cluster, followed by the formation of several intermediate structures through the successive cleavage of Sn–C bonds. In agreement with experimental data we found an oxidation state zero for the adsorbed Sn atom in the final structure, which is compatible, according to the adsorption geometry, with the coverage of 0.66 (Sn/Rh).

Keywords: geometry, electronic structure, $Rh_xH_ySn_z(CH_3)_n$

1. Introduction

Modern organometallic chemistry has had an enormous impact on homogeneous catalysis in the last two decades. Soluble metal complexes bind organic substrate molecules, which then undergo a large variety of transformations in the coordination sphere of the metal. The strategy for developing novel homogeneous as well as heterogeneous catalysts is based on the knowledge of the series of elementary steps that constitute the catalytic mechanism. This governs the choice of the central metal atom, its oxidation state, ancillary ligands and reaction conditions. Mechanistic studies carried out with well-defined organometallic complexes have identified key intermediates in many catalytic processes. However, the efficiency of homogeneous catalysts is often limited by instability caused by irreversible ligand dissociation and side reactions such as bimolecular reactions of unsaturated (highly reactive) intermediates. Separation and recovery of the catalyst, which sometimes contains an expensive metal such as Rh, is usually not efficient.

A recent development in catalysis, derived from surface organometallic chemistry involves the immobilization of the organometallic complex directly on a surface [1]. Site isolation and limited mobility of catalytically active molecules inhibit bimolecular decomposition reactions, and catalyst recovery becomes a simple matter of phase separation. An additional and considerable advantage is that unsaturated intermediates are readily formed and stabilized by the surface, which acts as a large and rigid ligand to trap them. Although the supported organometallic complexes superficially are heterogeneous catalysts, their relatively uniform structure, reactivity and distribution on the support material make them essentially homogeneous in nature.

The potential benefit to catalysis is now beginning to be realized. Catalyst active sites can be custom-designed with the ligand environment, oxidation state and other chemical properties desired for a given reaction. Any organometallic material can be used with a large variety of supports. The activity of these catalysts is often very high, since the concentration of active sites is controlled by the level of organometallic loading. In addition, the catalysts may possess enhanced selectivity usually associated with traditional homogeneous catalysts.

A representative structure with well-defined properties is obtained by means of the reaction of tetra(*n*-alkyl) tin with highly dispersed Rh metal (1.4 nm particle size) supported on silica, previously reduced under flowing H_2 at 673 K [2]. This gives a new generation of hydrogenation catalysts that selectively activate C=O bonds in the α,β unsaturated aldehyde hydrogenation reactions [3], and is associated with the general formula $Rh_xH_ySn_zR_n$. Organometallic modification of the Rh center has also shown to be promising for the molecular control of chemo-, regio- and enantioselectivity in Rh-catalyzed reactions. It has been demonstrated that the high chemoselectivity is directly related to the presence of organic fragments grafted onto the surface of the metallic particles. Moreover, depending on the experimental conditions, the reaction can either be intercepted at an intermediate stage or lead to the Sn/Rh alloy [4]. At 100°C, an organometallic fragment with the empirical formula $(SnR_2)H_yRh_x/SiO_2$ is present on the surface, as has been demonstrated by several characterization techniques [2]. Electron microscopy has revealed an increase in the average particle diameter to 2.2 nm,

consistent with the formation of one to two monolayers of alkyl tin on the Rh surface. Adsorption measurements, on the other hand, have shown that one third of the surface Rh atoms are still accessible for binding CO, whereas XPS, as well as Mössbauer spectroscopy, have identified the oxidation state of the organometallic fragment, which corresponds to ca. 75% Sn(II) or Sn(IV) and 25% Sn(0). These measurements, which are reported in ref. [2], have also demonstrated that each Sn atom has a carbon atom at 0.217 nm and two heavy neighbors (Sn or Rh) at 0.268 nm.

In spite of the experimental effort, the structural and electronic characteristics of these new materials are not known, and do depend, as the catalytic properties, on the conditions of the reaction synthesis. Research is oriented, though, not only to the knowledge of the electronic characteristics of the system, but also to understand their relation with its catalytic properties, looking for a way to design, on this basis, new materials of improved catalytic behavior.

Because of the importance of this subject, which not only opens a new field in catalytic research but also in organometallic synthesis, we are devoted to find an explanation, at an electronic level, of the fundamental mechanisms governing the different steps in the preparation and activation of Rh–SnR_n ($R = CH_3$) structures for low Sn/Rh ratios, i.e., the activation of the metallic cluster and its interaction with $Sn(CH_3)_4$ to give the final structure, with particular catalytic properties and selectivity.

We present, at this time, the results of quantum-chemical self-consistent field (SCF) calculations that, through the study of the structural, electronic and magnetic characteristics of the intermediates, and the energy associated with each step of the reaction synthesis, gave us some hints to understand the relation between the structural and electronic properties of the different structures and its catalytic activity. It is our hope that this might further help us to understand its particular selectivity.

2. Computational details

Highly dispersed catalysts, with particle size distribution in the order of nanometers [5], may be obtained through surface organometallic synthesis. From previous studies of the geometric and electronic characteristics of transition metal clusters as a function of the size [6], a larger stability of the icosahedral (I_h) symmetry compared to the cuboctahedral (O_h) or hcp (D_{3h}) ones, is known to characterize the small 13-atom clusters of materials that crystallize in fcc lattices.

Perfect I_h structures, whose planes resemble close-packed (111) planes, are based on a 13-atom-centered icosahedron. While a 55-atom icosahedron may better represent the actual particle size in supported clusters, a 13-atom icosahedron is the simpler one that keeps the same local properties on the active centers, because the local environment on each of the surface sites is identical to that of the larger 55-atom clusters. We have chosen, thence, this structure, to analyze, at the SCF-multireference-configuration-interaction level (intermediate neglect of differential overlap [7] INDO-MRCI) the interaction of Rh clusters with atomic hydrogen, resulting in the reduced substrate [8] which further reacts with $Sn(CH_3)_4$ to give the organometallic catalyst [9].

Calculations have been made at the restricted Hartree–Fock (RHF) and restricted open-shell Hartree–Fock (ROHF) levels.

The calculated geometries are the result of a full optimization of the coordinates (interatomic distances and angles) without any constraint in their variation. Optimization is based on a minimization of the gradient [10] evaluated analytically (INDO/1), using the BFGS algorithm to update the inverse Hessian matrix in successive cycles. The SCF calculations were followed by a CI using a Rumer diagram technique [11] within the INDO/S, parametrized against spectroscopic data [12].

Changes in the one-electron distribution during the SCF cycles in structures of high symmetry may lead to nonequivalent occupation of degenerated orbitals that, by breaking the symmetry in the electronic distribution, may result in spurious Jahn–Teller distortions. We have avoided this effect using configuration average Hartree–Fock (CAHF) theory [13] with an average multiplicity (M) for the number of electrons considered. The final M has been chosen after CI calculations, using the orbitals of the CAHF calculation as the reference for the Rumer CI projection over pure spin states [11].

Binding energy (BE) values are calculated as the difference between the total energy of the $Rh_{13}X$ structure and the sum of the total energies of the metal cluster Rh_{13} and the species X. Positive BE values imply coordination.

It is well known that the INDO method used here overestimates bonding energies [14,15], as most of the NDO methodologies do. To account for this, the SCF-CI BE values derived from INDO calculations have been corrected to match the data derived from experiment or higher level calculations. The strengths of the Rh–H, C–Sn and Rh–Sn bonds were corrected to agree with experimental data (bond length and bond strength) reported in ref. [16]. To this aim, calculations at the CI level have been performed for RhH_2, $Sn(CH_3)_4$ and a hypothetic Rh–Sn molecule. Corrections of 1.9, 3.2 and 5.9 eV, respectively, were found necessary. The strength of the C–Rh bond, on the other hand, was corrected in 2.5 eV [14], to match the data derived from other calculation procedures, as no experimental data was available.

In the first step, associated with the reduction of the naked Rh cluster, the energy involved in the formation of the Rh–H bonds was calculated [17]. During the further reaction of tetraalkyl tin with the reduced Rh

clusters, Rh–Sn bonds were formed and C–Sn bonds were broken in a synchronic mechanism that also leads to Rh–C bond formation in the calculation of the total BE. The strength of those interactions has been taken into account.

Because of the inherent intricacy structures associated with the different steps of the reaction under study, the interactions between the particles involved do not lead to bonds of the same strength, even when defined by the same atoms. In order to apply the corrections, the strengths of bonds were estimated from the atomic bond index matrix [18].

3. Results and discussion

3.1. Interaction of hydrogen with Rh_{13}

As the first step in the study of the mechanism involved in the synthesis of bi- and organometallic catalysts we have analyzed the interaction of a hydrogen atom with Rh_{13} clusters (figure 1). According to MRCI calculations, perfect icosahedral Rh_{13} clusters are high-spin structures (multiplicity, $M = 12$). Although Jahn–Teller distortions would break the symmetry lowering the M [6], we have not taken this effect into account, as the I_h Rh_{13} cluster is used in this research as a model of the largest ones that would be actually present on the support. The comparison of the binding energies for the adsorption of a hydrogen atom on the different sites defined in the I_h structure [8] indicates that it is stabilized in the highest coordinated sites, where its tetracoordination results in a spin quenching of the Rh_{13}–H structure to zero magnetic moment (table 1, figure 1c) [8]. Values in table 1 have been already corrected according to the overestimation of the Rh–H bond strength and the Wiberg index for each particular coordination.

On the basis of this result, a completely reduced structure would be constructed by means of the adsorption of one hydrogen atom on each of the hollow sites located in the center of each of the twenty faces of the Rh_{13} icosahedron (figure 2). Our calculations, which simultaneously optimize the coordinates of all the hydrogen atoms without any constraint, show that a $Rh_{13}H_{20}$ cluster is formed as a stable structure, and define a monolayer coverage by hydrogen atoms for the Rh_{13} I_h. The optimized Rh–H distance results in 1.803 Å (table 1). The stoichiometry of the structure $H/Rh = 1.538$ ($Rh_{13}H_{20}$) is in agreement with experimental results, which report a value of ca. 1.5 for hydrogen adsorption on Rh supported over highly dispersed SiO_2 or Al_2O_3 at 298 K [19].

The positive BE value per hydrogen atom in the reduced structure, which is similar to that associated to the adsorption of a single hydrogen atom (see table 1), allows us to discard a destabilizing effect due to lateral interactions in the first monolayer coverage. Following the trend already described for a single hydrogen atom adsorption, the magnetization of the cluster decreases, going from $M = 12$ for the naked structure to $M = 4$ for the monolayer coverage in the $Rh_{13}H_{20}$ structure. In spite of the well known misleading results that a Mulliken population analysis can lead to [20], this formalism is still in widespread use and renders, in this case, an acceptable description of the electronic effects related to hydrogen adsorption. It shows a charge transfer effect from the hydrogen atoms to the metallic cluster that results in a negative charge density on the Rh atoms, mainly concentrated on the atom in the center. The charge density distribution is compared in table 1 for the naked cluster, for different coordinated geometries of a

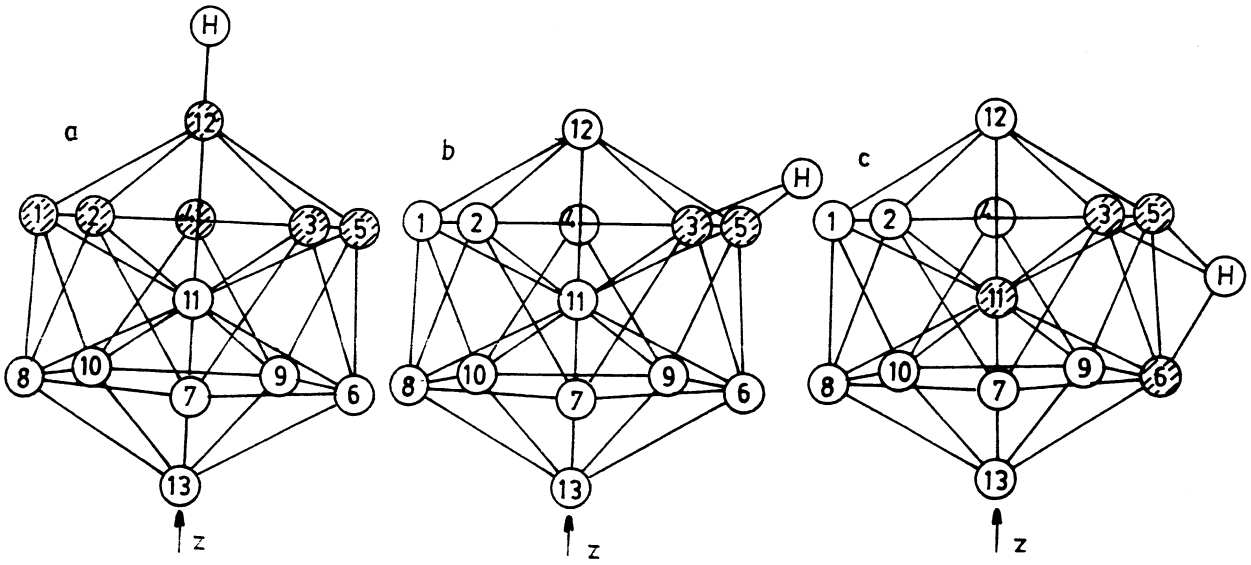

Figure 1. Coordination geometries of a single hydrogen atom on the Rh_{13} cluster. (a) Linear coordination (on top), (b) bicoordination (bridge), (c) four-fold coordinated (hollow).

Table 1
Binding energies (eV) per hydrogen atom, hydrogen adsorption distances R (Å) and local density charges on the hydrogen (q_H) and Rh atom (q_{Rh}) for the naked cluster, different coordination geometries of a single hydrogen atom and a monolayer coverage

	Rh_{13}	$Rh_{13}H$ on top	$Rh_{13}H$ bridge	$Rh_{13}H$ hollow	$Rh_{13}H_{20}$ hollow
Symmetry	I_h	C_{5v}	C_{2v}	C_{3v}	I_h
State	$^{12}T_{2g}$	$^{13}E_g$	$^{3}A_1$	$^{1}A_1$	$^{4}T_{1u}$
BE (eV)	–	1.898	2.005	2.780	1.830
R(Rh–H) (Å)	–	1.589	1.700	1.801	1.803
q_H		+0.243	+0.243	+0.260	+0.495 [c]
q_{Rh_1}	+0.281 [a]	+0.052	+0.088	+0.093	−0.648
q_{Rh_2}		+0.136	+0.095	+0.106	−0.708
q_{Rh_3}		+0.098	−0.046 [b]	−0.078 [b]	−0.672
q_{Rh_4}		+0.135	+0.095	+0.106	−0.708
q_{Rh_5}		+0.098	−0.047 [b]	−0.078 [b]	−0.672
q_{Rh_6}		−0.074	+0.048	−0.078 [b]	−0.648
q_{Rh_7}		+0.109	+0.071	+0.122	−0.708
q_{Rh_8}		−0.001	+0.137	+0.092	−0.672
q_{Rh_9}		+0.110	+0.071	+0.122	−0.708
$q_{Rh_{10}}$		−0.002	+0.137	+0.092	−0.672
$q_{Rh_{11}}$	−0.458	−0.886	−0.857	−0.990	−0.855
$q_{Rh_{12}}$		−0.286 [b]	−0.049	−0.122	−0.675
$q_{Rh_{13}}$		+0.267	+0.014	+0.106	−0.675

[a] Average density charge on each of the Rh atoms of the naked cluster.
[b] Rh atom bonded to a hydrogen atom.
[c] Average density charge on the H atoms in the $Rh_{13}H_{20}$ cluster.

single adsorbed hydrogen atom, and for monolayer coverage. The significant change in the charge distribution in the reduced particle, compared to the naked metal cluster, shows how the electronic characteristics of the active sites are modified by reduction.

3.2. Mechanism of the reaction between $Sn(CH_3)_4$ and the reduced cluster

The different steps involved in the mechanism of formation of the organometallic $Rh–Sn(CH_3)_n$ ($n = 4$–0) as result from the calculation, are depicted in figure 3.

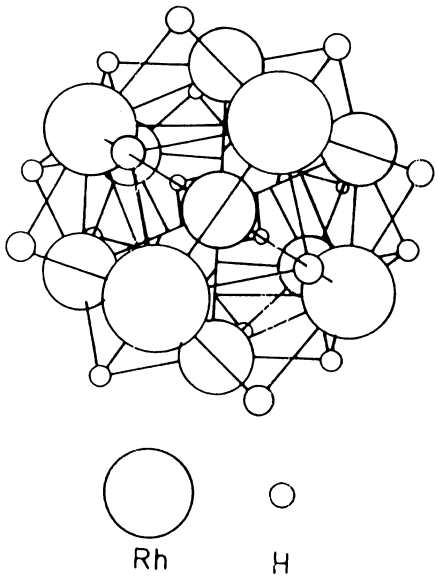

Figure 2. Monolayer coverage of the Rh_{13} cluster by hydrogen atoms.

We have found a preferential linear coordination of the $Sn(CH_3)_4$ molecule with a Rh atom of the reduced cluster, with simultaneous cancellation of unpaired spins to $M = 2$ (figure 3 b_1). Bi-coordination (bridge, figure 3 b_2), involving two adjacent Rh atoms bonded to Sn, generates a less stable intermediate. The linear Sn–Rh coordination weakens the Sn–C bonds associated to CH_3 groups non-adjacent to the $Rh_{13}H_{20}$ cluster, resulting in a preferred elongation of one of them (figure 3 b_1). The sticking of the Sn atom is helped by two CH_3 groups that are also involved in the adsorption, through coordination to adjacent Rh atoms. This process weakens the Sn–C bonds as well as the C–H bonds of the CH_3 groups bonded to the hydrogenated substrate, after coordination of the C atom with the Rh cluster. These changes in the bond strengths, quantified through the Wiberg indexes, has been considered in the BE calculation. The C–H bond order decreases from 0.98 in the free $Sn(CH_3)_4$ molecule to values between 0.34 and 0.89, depending on the interaction of the hydrogen atoms with the metal cluster.

The structure of the first intermediate adsorbed phase (figure 3 b_1), is the result of a geometry optimization of the $Sn(CH_3)_4$ adsorbate that also relaxed the apical Rh and the H atoms bonded to it. Optimization results in an elongation and simultaneous weakening of the Sn–C bond. On the basis of this result, we postulate a second step where the elongated Sn–C bond renders a CH_3 group which, through combination with a hydrogen atom that is also weakened after adsorption, evolves as

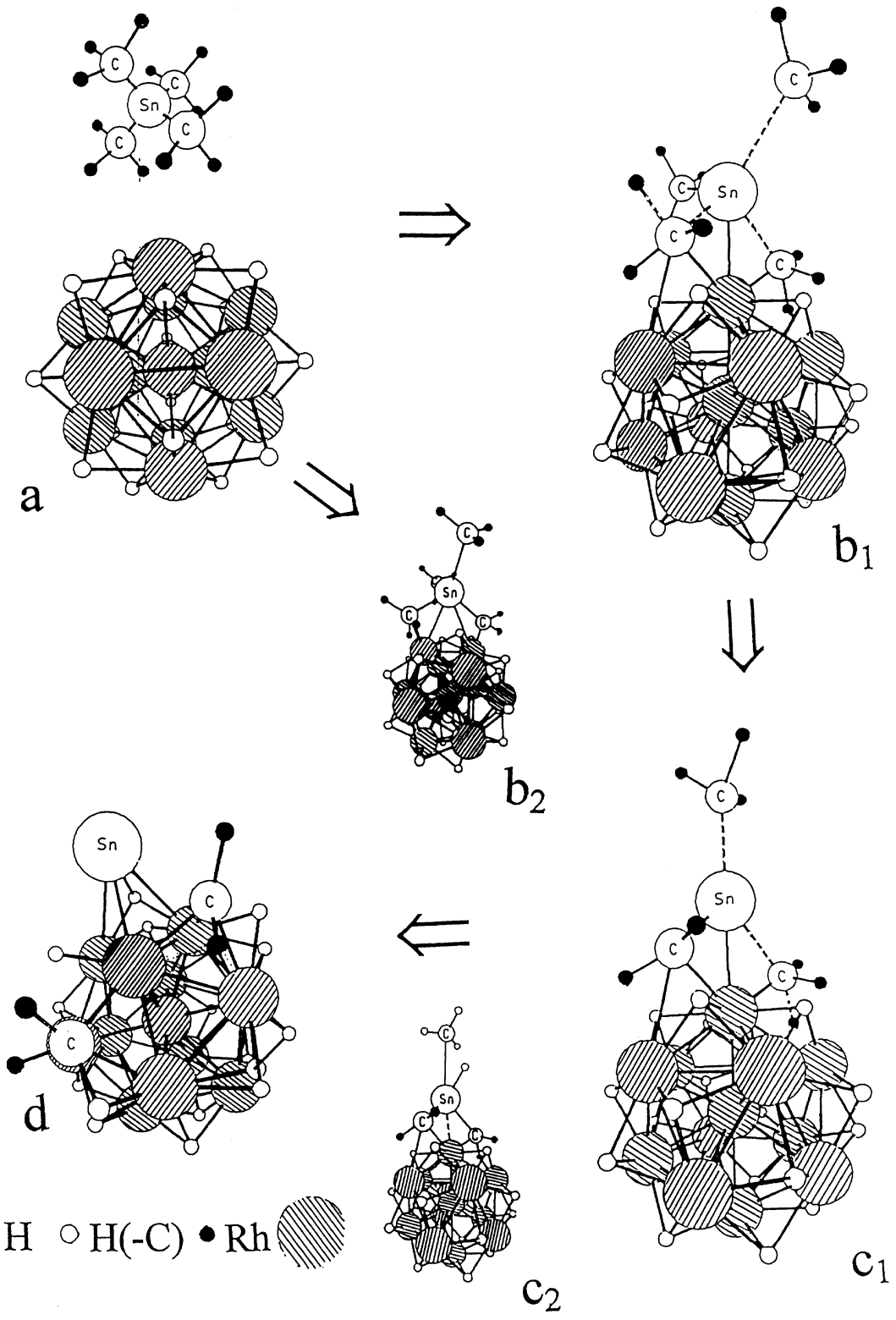

Figure 3. Structure involved in the different steps of the reaction between $Sn(CH_3)_4$ and the reduced $Rh_{13}H_{20}$ cluster: (a) before adsorption, (b) linear coordination of $Sn(CH_3)_4$ (broken lines show the bonds that are weakened). The structure actually represents an intermediate state that evolves to c_1, (c) intermediate structure that results from the loss of CH_4 (c_1) – broken lines show the bonds that are weakened and would be involved in the evolution to d, (d) final structure: two $-CH_2$ groups bonded to Rh atoms on a "quasi-bridged" coordination.

CH_4. In the intermediate structure thus generated (figure 3 c_1) the Sn atom is coordinated to a Rh atom and the three remaining CH_3 groups. Geometry optimization of this new structure leads again to a similar elongation of the Sn–C bond that involves the CH_3 group non-adjacent to the metallic cluster. We can postulate that another CH_4 molecule may be lost in a similar manner and a new intermediate compound may result whose stoichiometry corresponds to $Rh_{13}H_{20}Sn(CH_2)_2$ (figure 3d). The latter is better described as $(CH_2)_2Rh_{13}H_{20}Sn$, since the alkylic fragments are separated from the Sn and coordinate directly to superficial sites in a "quasi-bridged" coordination (intermediate between bridge and hollow). The Sn atom moves to a tricoordinated site and retains its characteristic tetracoordination through bonding to a reductor hydrogen that belongs to the $Rh_{13}H_{20}$ cluster. The resulting geometry is compatible with a Sn/Rh ratio 0.66, which has been found in experimental studies [2].

We have also investigated the alternate formation of a hydride intermediate structure of the type $Rh_{13}H_{20}Sn(CH_2)_2(CH_3)H$ (figure 3 c_2), but this possibility was discarded on the basis of energetic considerations.

In figure 4 the calculated energy changes associated to each step of the mechanism are shown. The reaction does not imply any change of M from the initial to the final structure.

Mulliken population analysis shows an orbital population 1.65 s 1.96 p on the Sn atom adsorbed of the final structure. Based on the electronic configuration of the neutral atom ($5s^2 5p^2$) it can be assigned to a zero oxidation state (Sn^0) with partial charge transfer to the reduced substrate, a result that is again in agreement with XPS, Mössbauer and kinetic experimental results [2,21].

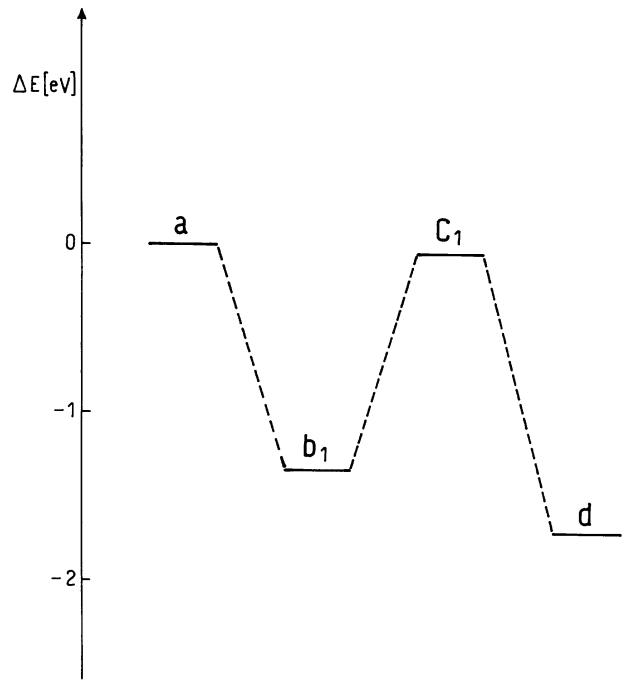

Figure 4. Energies associated to the different steps of the reaction between $Sn(CH_3)_4$ and the reduced $Rh_{13}H_{20}$ cluster. The structures associated to each step are shown in figure 3.

The proposed mechanism allows us to infer that the highest coverage compatible with our final structure should be associated to the occupation of three hollow sites (from the twenty available) for each alkyl tin molecule adsorbed, one for the Sn atom and one for each CH_3 group. This leads to a coverage of 0.66, in good agreement with the experimental value (2/3) determined through CO dosage [2].

There are several factors that, in some cases, cannot be neglected in order to get calculated energies closer to reality, as it is, for example, the effect of the support. However, for the system we are dealing with, experimental evidence has shown that the influence of the support does not seem to be relevant. In the case of the reaction between $SnBu_4$ and Rh, that occurs over a support, both the characteristics of the phase $Rh(SnBu_x)_y$ (ca. $x = 0$–2; $y = 0.0$–0.8) and the reaction mechanism for its formation are similar over SiO_2 and γ-Al_2O_3 supports [21]. Moreover, the activity of the SnRh phase towards the hydrogenation of ethyl acetate to ethanol is the same over both supports [22].

Other factors, as the size of the Rh cluster itself, or the coordination of the hydrogen atoms that may be shifted by coadsorption to intermediate positions also add severe complications for the overall picture, and lead to the definition of the system not able to be analyzed by quantum-chemical methodologies. We consider this calculation a first step that is mainly focused on the structure of the organometallic phases, being aware that the kinetics associated with the different steps, because of its complexity, may be not properly described at this level of calculation.

4. Conclusions

Based on geometry optimization procedures and electronic structure SCF(CI) calculations, the analysis of the steps involved in the interaction between a $Sn(CH_3)_4$ molecule and a reduced Rh_{13} I_h cluster shows that the mechanism implies the initial adsorption of alkyl tin to one Rh atom of the hydrogenated metal cluster, followed by the formation of different intermediates through the successive cleavage of Sn–C bonds.

A hydride structure of the type $Rh_{13}H_{20}Sn(CH_3)H$, is discarded as a possible intermediate of the proposed mechanism on the basis of energetic considerations.

The proposed mechanism shows that the Sn atom retains its tetracoordination through the occupation of a hollow site with simultaneous coordination of a hydrogen atom after detachment of the alkyl groups.

In agreement with experimental data we found a possible coverage of 0.66 (Sn/Rh) and an oxidation state zero for the former adsorbed Sn atoms in the final structure.

The study of the influence of the Sn coverage on the reaction mechanism and the modification of the final structure as a function of the coverage are the matter of present research in our lab. The results will be presented in a forthcoming article.

Acknowledgement

A.H.J. is a member of the Research Career of CIC, G.L.E. and O.A.F. are members of the Research Career of CONICET. The financial assistance of the Consejo Nacional de Investigaciones Científicas y Técnicas (CONICET), the Comisión de Investigaciones Científicas (CIC), Provincia de Buenos Aires and the Fundación Antorchas (Argentina), is gratefully acknowledged. This work has been made within the CYTED program.

References

[1] J.M. Basset, B.C. Gates, J.P. Candy, A. Choplin, M. Leconte, F. Quignard and C.C. Santini, *Surface Organometallic Chemistry: Molecular Approaches to Surface Catalysis* (Kluwer, Dordrecht, 1988).

[2] B. Didillon, C. Houtman, J.P. Candy and J.M. Basset, J. Am. Chem. Soc. 115 (1993) 9380;
S.L. Scott, J.M. Basset, G.P. Nicolai, C.C. Santini, J.P. Candy, C. Lecuyer, F. Quignard and A. Choplin, New. J. Chem. 18 (1994) 115.

[3] B. Didillon, J.P. Candy, F. Lepeltier, O.A. Ferretti and J.M. Basset, Stud. Surf. Sci. Catal. 78 (1993) 203;
B. Didillon, A. El Mansour, J.P. Candy, J.P. Bournonville and J.M. Basset, Stud. Surf. Sci. Catal. 59 (1991) 137.

[4] A. El Mansour, J.P. Candy, J.P. Bournonville, O.A. Ferretti, G. Mabilon, J.M. Basset, Angew. Chem. Int. Ed. Eng. 28 (1989) 347;
O.A. Ferretti and M.L. Casella, Lat. Appl. Res. 25 (1995) 125.

[5] J.M. Basset, J.P. Candy, P. Louessard, O.A. Ferretti and J.P. Bournonville, Wiss. Zeitschr. THLM 32 5/6 S (1990) 657;
O.A. Ferretti, J.P. Bournonville, G. Mabilon, G. Martino, J.P. Candy and J.M. Basset, J. Mol. Catal. 67 (1991) 283.

[6] (a) G.L. Estiú and M.C. Zerner, Int. J. Quantum Chem. 27 (1993) 195;
(b) G.L. Estiú and M.C. Zerner, J. Phys. Chem. 98 (1994) 4793;
(c) G.L. Estiú and M.C. Zerner, J. Phys. Chem. 98 (1994) 9972.

[7] M.C. Zerner, ZINDO package, Quantum Theory Project, Williamson Hall, University of Florida, USA.

[8] M.C. Michelini, A.H. Jubert and G.L. Estiú, J. Mol. Struct. THEOCHEM 335 (1995) 153.

[9] M.C. Michelini, G.L. Estiú, A.H. Jubert and O. Ferretti, Información Tecnológica 7 (1996) 147.

[10] (a) A. Szabo and N.S. Ostlund, *Modern Quantum Chemistry. Introduction to Advanced Electronic Structure Theory* (Mc Graw Hill, New York, 1989);
(b) J.D. Head and M.C. Zerner, Chem. Phys. Lett. 122 (1985) 264;
(c) J.D. Head and M.C. Zerner, Chem. Phys. Lett. 131 (1986) 359.

[11] R. Pauncz, *Spin Eigenfunctions* (Plenum Press, New York, 1979).

[12] W.D. Edwards and M.C. Zerner, Theoret. Chim. Acta 72 (1987) 347.

[13] M.C. Zerner, Int. J. Quantum Chem. 35 (1989) 567.

[14] G.L. Estiú and M.C. Zerner, Int. J. Quantum Chem. 26 (1992) 587.

[15] M.C. Zerner, in: *Reviews in Computational Chemistry*, Vol. 2, eds. K.B. Lipkowitz and D.B. Boyd (VCH, New York, 1990).

[16] D.R. Lide, ed., *CRC Handbook of Chemistry and Physics* (CRC Press, Boca Raton, 1990–1991).

[17] M. Michelini, A.H. Jubert and G.L. Estiú, J. Mol. Struct. THEOCHEM 335 (1995) 153.

[18] K.B. Wiberg, Tetrahedron 24 (1968) 1083.

[19] J.P. Candy, A. El Mansour, O.A. Ferretti, G. Mabilon, J.P. Bournonville, G. Martino and J.M. Basset, J. Catal. 112 (1988) 201.

[20] S.M. Bachrach, in: *Reviews in Computational Chemistry*, Vol. 5, eds. K.B. Lipkowitz and D.B. Boyd (VCH, New York, 1994).

[21] O.A. Ferretti, C. Lucas, J.P. Candy, J.M. Basset, B. Didillon and F. Le Peltier, J. Mol. Catal. 103 (1995) 125.

[22] O.A. Ferretti, PhD Thesis, Université Paris VI, France (1986).